Ion Binding Constants for Gramicidin A Obtained from Water Permeability Measurements

K.-W. Wang[1,*], S. Tripathi[2], S. B. Hladky[1]

[1]Department of Pharmacology, University of Cambridge, Cambridge CB2 1QJ, United Kingdom
[2]Tata Institute of Fundamental Research, Colaba, Bombay, 400-005, India

Abstract. Gramicidin A pores are permeable to water and small monovalent cations. For K, Rb, and Cs there is good evidence from conductances and permeability ratios that a second ion can enter a pore already occupied by another, but for Na this evidence is inconclusive and comparison of tracer fluxes and single channel conductances suggests that second ion entries are prohibited. Partly as a result of the complications of second ion entry there have been widely differing estimates for the dissociation constants for the first ion in the channel. Dani and Levitt (1981, *Biophys. J.* **35:** 485–499) introduced a method for calculating ion binding constants from simultaneous measurements of water fluxes and membrane conductance. They found no evidence for second ion binding and calculated dissociation constants of 115 mM for Li, 69 mM for K, and 2 mM for Tl. It is shown here that the two-ion, four-state model predicts a dependence of water permeability on ion concentration that is difficult to distinguish from the predictions of block by a single ion. Using a modified technique that allows measurement of higher conductances, the first ion dissociation constants have been determined as 80 mM for Na, 40 mM for Rb and 15 mM for Cs. These values and those of Dani and Levitt fall in a smooth sequence. The dissociation constant for Cs is consistent with single channel conductances and flux ratios. There is a discrepancy between this constant for Na and the value, 370 mM, calculated from the single channel conductances and the assumption that a second ion cannot enter or affect an occupied pore. The dissociation constant for Rb is inter-

mediate between those for K and Cs whereas tracer flux measurements (Schagina, Grinfeldt & Lev, 1983. *J. Membrane Biol.* **73:** 203–216) have suggested that Rb interacts much more strongly with the channel than Cs.

Introduction

Gramicidin A pores are permeable to small monovalent cations and water. The mechanism of conduction has been described using a four-state, two-ion model (Hladky, 1972, 1988; Urban & Hladky, 1979; Finkelstein & Anderson, 1981, Hladky & Haydon, 1984) in which the transport is assumed to occur as a result of five distinguishable processes: entry of an ion to a pore occupied only by water, transfer of an ion through the pore, exit of an ion when one is present, entry of a second ion, and exit of either ion when two ions are present. Each of these processes is in turn described by a rate constant which may vary with potential but not ion concentration. Using this model gramicidin conductances measured with symmetrical solutions (Hladky & Haydon, 1972; Neher, Sandblom & Haydon, 1978; Urban, Hladky & Haydon, 1980) are consistent with a range of values of the rate constants (Hladky & Haydon, 1984). Simultaneous fitting of conductances and permeability ratios (Urban et al. 1978, 1980) produced one fit in which exit from singly occupied pores is much slower than transfer and another in which these rates are comparable. Fitting to the conductance-activity curves alone (Hladky & Haydon, 1984) produced intermediate values.

The first set of constants is consistent with the slow off rate for Na inferred from NMR spectra for gramicidin

* *Present address:* Boyer Center for Molecular Medicine, Yale University School of Medicine, 295 Congress Avenue, New Haven, Connecticut 06536-0812

Correspondence to: S.B. Hladky

in lysophosphatidylcholine dispersions (Monoi, 1985; Hinton et al., 1986, Urry et al., 1989). However, flux ratio measurements for Cs and Na in either diphytanoylphosphatidylcholine membranes (Procopio & Andersen, 1979; Andersen, 1984) or monoglyceride membranes (M. Jones, D.S. Game, S.P. Moule and S.B. Hladky, *unpublished observations*) suggest that exit is more rapid. Those for Na have been taken to imply that second ion entries by Na are impossible (Finkelstein & Andersen, 1981). In contrast, flux ratio data obtained using bull-brain lipids (Schagina et al., 1978, 1983) imply for these negatively charged membranes and Rb that second ion entries are even more important than expected from the earlier fits. The failure of Na ions to block currents carried by hydrogen ions (Heineman & Sigworth, 1989) argues for relatively rapid exit of Na ions from the pore.

Dani and Levitt (1981) reported that Li, K, and Tl ions reduce the osmotic water permeability of gramicidin pores. They found that their data could be described by block of the pore by binding of a single ion,

$$P_{wc} = \frac{P_o K_D}{K_D + c} \tag{1}$$

where P_o is the water permeability of a channel without an ion, P_{wc} is the open-circuit permeability at ion concentration, c, and K_D is the dissociation constant for the ion. The values they found for the K_D were intermediate between the two sets of constants found by Urban et al. (1980). They saw no evidence for binding of a second ion.

We report here the theoretical prediction of the two-ion, four-state model and the use of an extension of the technique introduced by Dani and Levitt to obtain estimates of the first ion binding constants for Na, Rb, and Cs ions in gramicidin pores. These values and those reported by Dani and Levitt fall into a smooth sequence. Our value for the water permeability at low ion concentrations is at least as large as that reported by Dani and Levitt.

The theoretical expression for the water permeability of a pore described by the two-ion, four-state model has been stated previously in an abstract (Hladky, 1983).

Materials and Methods

Membranes were formed from glyceryl mono-oleate (NuChek Prep, Elysian, MN) dissolved at 10 or 20 mg/ml in *n*-hexadecane (Koch-Light, puriss). The *n*-hexadecane was passed through an alumina column prior to use to remove polar impurities. Gramicidin A (gift of E. Gross, NIH) was added from stock solutions in ethanol (absolute, AR grade, BDH, Poole, UK). Salt solutions were prepared using Analar (NaCl, CsCl, MgCl₂) or technical grade (RbCl from BDH, Poole, UK) salts and water obtained from a commercial still modified by the replacement of all plastic tubing with Teflon and borosilicate glass. Salts were roasted at ~500°C prior to use to remove organic impurities.
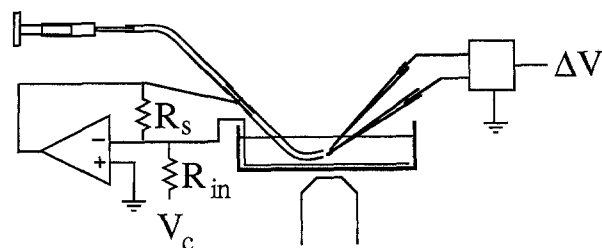

Fig. 1. Diagram of the apparatus used for the simultaneous measurement of volume flow and membrane conductance. A syringe is attached to a length of teflon tubing which is interrupted by a short length of silver tubing. The syringe and tubing make up the inner compartment. The outer compartment is a tissue culture dish. The membrane is formed across the mouth of the tube and current across the membrane $(=V_c/R_{in})$ is controlled by a feedback amplifier. The shunt resistor provides a pathway for the input bias current when the membrane is nonconducting. The potential difference, ΔV, between two points in the solutions is measured using two microelectrodes.

In experiments with 1 or 10 mM NaCl or CsCl, the solutions also contained 5 mM MgCl₂ to reduce solution and electrode resistances. Solutions containing urea (cell culture grade, Sigma Chemical, Poole, UK) were prepared by adding solid urea to an aliquot of the salt solution of the experiment. Thus, the molality of the salt was the same with or without the added urea. All experiments were conducted at room temperature, typically 22°C.

Patch pipettes used for measuring potentials were pulled from 1.2 mm OD filamented borosilicate glass capillaries (GC120F-10; Clark Electromedical Instruments, Pangbourne Reading, England) using a PP-83 puller (Narishige Scientific Instrument Laboratory, Tokyo, Japan). The pipettes were vapour phase silanized using a 10:1 chloroform dilution of dimethyldichlorosilane (Sigma) as described by Wang and Hladky (1994). Pipettes were back-filled with a filtered (Millex-GS, 0.22 μ, Millipore) aliquot of the aqueous solution used to fill the Teflon tubing. When filled with a low permeant ion concentration plus 5 mM MgCl₂, the pipette resistance was ~10⁷ Ω. Blockage of the microelectrode tip by lipid during membrane crossing was cleared by applying brief pressure pulses to the sidearm of the microelectrode holder.

The apparatus is shown in Fig. 1. A 100 μl Hamilton gastight syringe fitted with a micrometer drive is connected to Teflon tubing interrupted by a short length of silver tube (99.9%, 2 mm OD, Goodfellows Metals, Cambridge, UK). The final portion of tubing has an OD of ⅛" and ID of 1/16" (FEP, 6406-62, Cole Parmer Instruments, Chicago). The silver tubing, chloridized on the inside, serves as the inner current electrode. The outer cell, a 60 mm disposable tissue culture dish is placed on the stage of an inverted microscope (Nikon, TMS). The outer current electrode is a length of chloridized silver wire (also 99.9%) which follows the circumference of the dish. The inner current electrode is attached to the output of the current source (AD744J amplifer, Analogue Devices, Norwood, MA). The outer current electrode is connected to the virtual earth input and to the input resistor, R_{in}. This resistor can be selected with a switch to be 10³, 10⁴, 10⁵, or 10⁸ Ω. A 10⁸ Ω shunt resistor is provided to prevent the input bias current from producing a large potential across the membrane before the addition of gramicidin. It has no effect during the conductance measurements as the membrane cell then has a resistance of less than 10⁵ Ω. Potential differences are measured using two, patch clamp electrodes which can be positioned near to the membrane with micromanipulators. The microscope and the manipulators are mounted on an air table (AVT 700, Wentworth Laboratories, Bedford, UK).
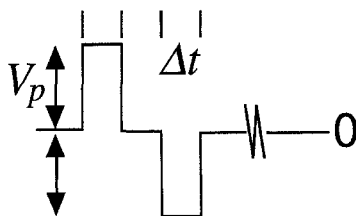
Fig. 2. The voltage waveform applied to the current clamp. The pulses are of equal duration and magnitude, but opposite sign. This procedure minimizes solution polarization resulting from the passage of the current.

The signals from the electrodes are fed via 2× voltage followers (AD711J) with positive capacitative feedback for frequency compensation into a 1× differential amplifier (AD744J). The resistors that determine the gain of the followers and the four resistors that determine the gain and common mode rejection of the differential amplifier are nominal 0.1% tolerance. The overall common mode signal was measured to be less than 0.5 mV for a 4 V common input to the followers. The virtual earth of the current clamp is connected to the outer, low resistance electrode to minimize common mode voltages and avoid saturating the voltage followers. Paired positive and negative potential pulses (*see* Fig. 2) were applied to the input of the current clamp at intervals and the responses to the current pulses were displayed on and read from the screen of a variable persistence storage oscilloscope (Tektronix 5441 with 5A22N amplifiers).

Membrane capacitance in the absence of gramicidin ($R_s C_m > 0.1$ sec) was measured by applying 5 V, 10 msec pulses with $R_{in} = 10^8$ Ω. The potential difference across the membrane (equal to that across the current electrodes for such small currents) increased linearly with time during the positive pulse, remained constant between the pulses, and returned to the baseline during the negative pulse. The capacitance could then be calculated from the measured potential change, ΔV, as

$$C = \frac{5V \times 10 \text{ msec}}{10^8 \ \Omega \times \Delta V} .$$ (2)

Areas were calculated as $C/5.8$ nF mm^{-2} (Andrews, Manev & Haydon, 1970).

At the start of the experiment the syringe and tubing were filled with the salt solution (without urea), and a known volume of the salt solution was pipetted into the outer dish. A drop of the lipid solution was placed at the end of the tubing and partially bulged outwards by advancing the syringe. Part of the lipid plug was then removed either by careful suction with a pipette or by passing air bubbles across its surface. The resulting film was bulged outwards so that its point of furtherest protrusion could be viewed tangentially through the inverted microsope. If any membrane movement was observed at this stage, the experimental setup was checked for leaks; no experiment was continued if there was a drift in membrane position. (Our limit of resolution is about 0.5 nl in 10 min). The membrane was bulged to a standard area (usually 4.2 mm^2) and the membrane reference position noted. Gramicidin was then added to the external solution in amounts ranging from 5 µl of a 10^{-5} M stock to 30 µl of a 10^{-3} M stock.

At least 5 min after adding gramicidin, concentrated urea solution (1 M for 200 or 500 mM final concentration, 2 M for 1 M final concentration) was added to the outer solution in two aliquots. The final urea concentration had to be high enough that the changes in salt concentration were relatively small by comparison. However, higher concentrations and the resulting higher volume flows produce greater concen-

tration changes. The control flow produced by 200 mM urea was easily resolved, thus there was no need for higher flow *per se*. The highest urea concentration was used only for the 1 M and some of the 500 mM Na points. The solution was mixed by withdrawing part of the solution into the Gilson tip and expelling it so as to produce alternatively clockwise and counterclockwise movement of the contents of the dish. This process produced complete mixing within 1 min of the start of the addition. The water flow started early in the addition and was usually stable from the end of the addition until the completion of the experiment (typically more than 10 min). The membrane conductance was usually measured just before the addition of urea, and about 4 min after. The number of channels is calculated from the latter value. In control experiments only a small amount of gramicidin was added, sufficient to make the membrane selectively permeable to the cation yet insufficient to increase the water permeability.

Other than during the application of pulses, the current across the membrane was clamped to zero by applying zero voltage to the 10^8 Ω input resistor, and the zero-current potential at the output of the clamp noted at regular intervals. After addition of the gramicidin, the microelectrodes were positioned outside the membrane with one tip ~5 µm closer to the membrane than the other. The input resistor was then chosen between 10^5 and 10^3 Ω, V_p was chosen between 100 mV and 4 V, the current pulses, ΔI, were applied, and the change in potential between the electrode tips was measured for the current change from $+\Delta I$ to $-\Delta I$. The input capacity compensation was adjusted at this stage to yield the squarest possible response to the step change in current. The membrane was then advanced until it crossed the tip of the closer microelectrode, the electrode was cleared with a pressure pulse, and the measurement was repeated. The difference between the two measurements was taken to be the potential difference across the membrane for a current of $2\Delta I$. This cycle was repeated several times to ensure that the value was reproducible. It was important not to change the separation of the electrode tips so as not to change the resistance of the solution between them[1]. It was also important to use brief pulses (<10 msec for $I < 0.4$ mA, <3 msec for 0.4 mA $< I < 4$ mA) to avoid polarization effects during the test pulses.

Results

As in previous papers (Rosenberg & Finkelstein, 1978; Dani & Levitt, 1981), the number of gramicidin channels, N, is calculated from the conductance of the membrane, G, and the single channel conductance, g, as $N = G/g$. We have used the value of g interpolated to the geometric mean of the concentrations at the two ends of the channel (*see below*) using the rate constants for fit G-c (Hladky & Haydon, 1984). The control or background permeability of the membrane is calculated as

$$P_w = \left(\frac{dV}{dt}\right)_{\text{control}} \bigg/ A\overline{V}_w \Delta C_{\text{osm}}$$ (3)

and the water permeability of a single channel, P_{wc}, is calculated as

---

[1] The two solutions have different resistivities. Thus, for large tip separations the jump size was a function of the membrane position between the tips.
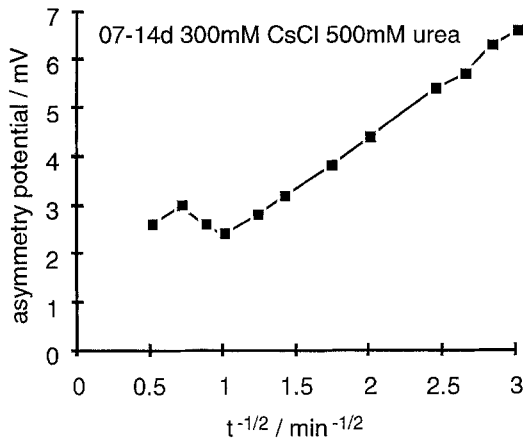
Fig. 3. The zero-current potential develops linearly with the square root of time.

$$P_{wc} = \frac{\left(\dfrac{dV}{dt}\right)_N - P_w A \overline{V}_w \Delta C_{osm}}{N \overline{V}_w \Delta C_{osm}} \qquad (4)$$

where $(dV/dt)_{control}$ is the rate of change of volume for low gramicidin (100-fold less added than needed to increase the volume flow), $(dV/dt)_N$ is the rate of change with N channels present, $\overline{V}_w$ is the partial molar volume of water, ΔC_{osm} is the difference between the osmolarities of the solutions adjacent to the two surfaces of the membrane (*see below*) and A is the membrane area. For rate of change in volume in cm^3/sec, area in cm^2, osmolarity difference in mol/cm^3, and partial molar volume in cm^3/mol the single channel permeability is in cm^3/sec.

The flow through the solutions and across the membrane changes the concentrations of solutes at the membrane surfaces. At the inside surface the volume flow brings up water and salt, only the water crosses the membrane, and the salt concentration increases. At the outer surface, the volume flow away from the membrane will tend to reduce the concentrations of salt and urea. As argued by Dani and Levitt (1981), the changes occur primarily at the inside surface and can be estimated from the increase in zero current potential that is observed after the osmotic flow commences (Levitt, Elias & Hautman, 1978). For diffusion from a semi-infinite medium (the solution in the tube) the expected dependence is the sum of a jump, partly resulting from the streaming potential, and a component which increases proportionally with the square root of time. This pattern was observed by Levitt et al. (1978) and in the present study (Fig. 3). The varying component, $\Delta V_{measured}$, is the sum of two terms, a positive term, ΔV_{conc}, representing the change in the ratio of the permeant cation concentrations at the two surfaces of the membrane, and a small negative term,

$\Delta V_{streaming}$, representing the decrease in the streaming potential and the measured varying component which results from the decrease in the osmotic driving force. For Na there is also a diffusion potential in the inner solution that results because the Na and Cl diffusing away from the membrane have unequal mobilities.

The concentration of the permeant at the inside mouth of the channel has been calculated as

$$C_m = C_{salt} e^{\frac{F \Delta V_{conc}}{RT}} \qquad (5)$$

and the osmolarity difference as

$$C_{osm} = C_{urea} - (2C_{salt} + 3C_{MgCl_2}) \left(e^{\frac{F \Delta V_{conc}}{RT}} - 1 \right). \qquad (6)$$

with

$$\Delta V_{conc} = \Delta V_{measured} + n \times (0.45 \text{ mV}) \times C_{osm}/(1 \text{ M}) \qquad (7)$$

In Eq. (7) values of n, the number of water molecules transported per ion, have been taken from Levitt (1984). For Na, the result of Eq. (7) has been divided by 1.2 as an approximate correction for the presence of the diffusion potential. (The ratio of the diffusion potential to the true concentration potential across the membrane is approximately equal to the difference in the transference numbers for Cl and Na which is ~0.2).

The control water permeability was $4.9 \pm 0.2 \times 10^{-3}$ cm sec^{-1} (mean $\pm$ SEM for 11 determinations, 4.4 ± 0.2 uncorrected). Figure 4 reports the calculated single channel permeabilities measured with Cs, Rb, and Na. For low ion concentrations, the major correction occurs via the effect of the change in the permeant ion concentration on the single channel conductance. For high ion concentrations, the major correction is a reduction in the osmotic gradient. In all of the experiments reported here the volume flow was the same both before and after determination of the membrane conductance. We have usually not observed the decrease in water flow with time that is predicted by the corrections. For this reason and to indicate the effect of the corrections, we also report the uncorrected values calculated with g interpolated to the bulk concentration and C_{osm} equal to C_{urea}. The slope of the plot of potential *vs.* the square root of time increased with volume flow and was less for higher ion concentrations (*see* Fig. 5 for Cs, similar results were obtained with Na).

Discussion

For K, Rb, and Cs more than one ion can bind to the pore. Thus, it is not obvious that a simple binding relation can be used to analyze the data. The two-ion, four-state model predicts a more complicated relation for the
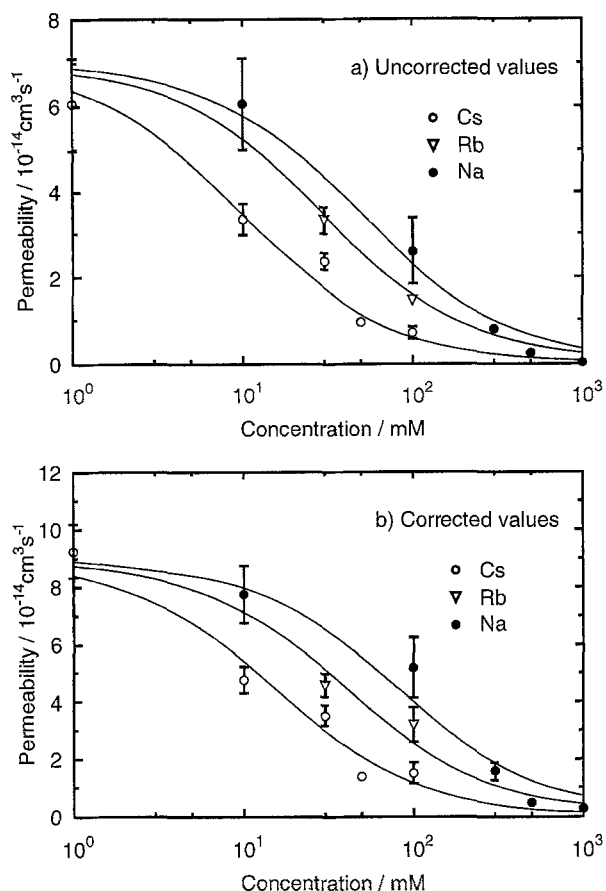
Fig. 4. Single channel water permeability *vs.* the concentration of the permeant ions. For the uncorrected values the number of channels, N, is estimated as the measured conductance divided by the single channel conductance for the indicated concentration. The permeability is then calculated as (measured water flow minus control)/C_{urea}/N. For the corrected values, the number of channels is calculated using the single channel conductance for the geometric mean of the surface concentrations and C_{urea} is replaced by the calculated difference in total solute concentrations across the membrane, C_{osm}. Error bars are SEM. Where not shown they are smaller than the symbol (for 1,000 mM Na, there were only two successful experiments). The curves are calculated using

		Uncorrected	Corrected
$P = \dfrac{P_o K_D}{K_D + c}$	$P_o/(10^{-14}\ \text{cm}^3\text{sec}^{-1})$	7	9
	$K_{D,Cs}/(\text{mM})$	10	15
with values	$K_{D,Na}/(\text{mM})$	50	80
	$K_{D,Rb}/(\text{mM})$	30	40

open circuit ($I = 0$) water permeability of the pore (*see* Appendix)

$$P_{wc} = P_o X_{00} \Delta C_{osm}$$

$$+ (\eta_s - \eta_d)^2 \frac{ADc^2}{2\mathscr{A}(B + Dc)} \overline{V}_w \Delta C_{osm} X_{00}$$

$$+ (\eta_d' - \eta_d'') \frac{AD}{2\mathscr{A}B} c^2 X_{00} \tag{8}$$
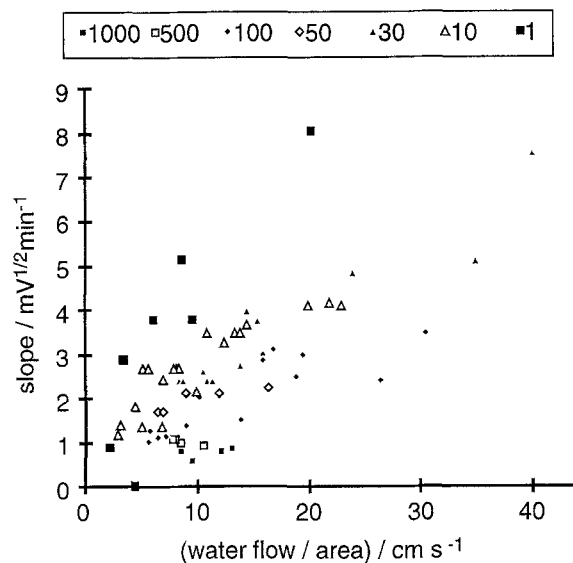

Fig. 5. The slope of the measured zero-current potential *vs.* the square root of time curve plotted *vs.* water flow. CsCl at the concentrations in mM indicated by the symbols. The slopes are roughly proportional to flow, but for the same flow are much smaller for high ion concentrations. All available data are presented including controls (low gramicidin).
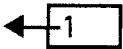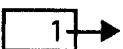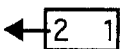
where $\mathscr{A}$ is Avogadro's number, A to E are rate constants in the model (see the Table, $K_D = B/2A$), c is the permeant ion concentration, X_{00}

$$X_{00} = \frac{1}{1 + \dfrac{2A}{B}c + \dfrac{AD}{BE}c^2}. \tag{9}$$

is the probability the pore does not contain an ion, and η_s and η_d are the number of water molecules that accompany an ion which crosses by the one-ion and two-ion modes, respectively.

The first term in this relation, which corresponds to the full expression used by Dani and Levitt (1981), represents the movement of water through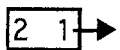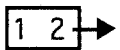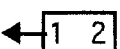 pores that do not contain ions. Taken alone, this term predicts that initially as the ion concentration is increased the permeability will fall as expected for block by a single ion, but at higher concentrations second ion binding will decrease the permeability further. The second and third terms describe water flow that occurs even if the pores are almost always occupied by an ion. The second term represents a net flux of water that can occur because ion transport can proceed by either the one-ion or the two-ion modes. This water flux is associated with a circulation of ions going in one direction by one mode and returning by the other. The water flux and the circulation of ions are driven by the osmotic gradient. The circulation does not violate microscopic reversibility because the system is

Table 1. The possible transitions in the "four-state" pore modified to allow for the presence of an osmotic gradient[a]

Ion transition	Schematic	Rate constant	Number of water molecules leaving right end of pore
Entry from left to empty pore	(diagram)	A'	η'_A
Exit to left from singly occupied pore	(diagram)	B'	$-\eta'_A$
Entry from right to empty pore	(diagram)	A''	$-\eta''_A$
Exit to right from singly occupied pore	(diagram)	B''	η''_A
Transfer from left to right	(diagram)	k'	η_k
Transfer from right to left	(diagram)	k''	$-\eta_k$
Entry from left to singly occupied pore	(diagram)	D'	η'_D
Exit to left after a second ion enters from left	(diagram)	E'	$-\eta'_D$
Exit to right after a second ion enters from left	(diagram)	$E''*$	η''_D*
Entry from right to singly occupied pore	(diagram)	D''	$-\eta''_D$
Exit to right after a second ion enters from right	(diagram)	E''	η''_D
Exit to left after a second ion enters from right	(diagram)	$E'*$	$-\eta'_D*$

[a] Whenever an ion moves there are also movements of water molecules. The rate constants and water movements when ions leave doubly occupied pores depend upon the order in which the ions entered because the number of water molecules trapped between them may depend on the osmolality of the side to which the center was last exposed.

not at equilibrium. The third term represents a net flux of water that will occur if the number of water molecules trapped between two ions in the pore is different when the second ion enters from the left or the right. Alter-nating left and right entries and exits can then lead to a net water flux. The difference $\eta'_d - \eta''_d$ should increase with increases in ΔC_{osm}.

For $P_o = 9 \times 10^{-14}\,cm^3\,sec^{-1}$, $\Delta C_{osm} = 10^{-3}\,mol\,cm^{-3}$

and differences, $\eta_s - \eta_d = 2$ and $\eta'_d - \eta''_d = 1$ the second and third terms are appreciable only for high permeant ion concentrations, $Ac,Dc > B$. However, these high concentrations are also expected, $Dc > E$, to affect the first term by second ion binding. These effects should partially cancel. Unfortunately, neither the present data nor that reported by Dani and Levitt for high ion concentrations are sufficiently accurate to provide a test. Over the range of data available, this relation cannot be distinguished from the relation for block by a single ion.

In the experimental technique described by Dani and Levitt (1981) potential changes were measured between a microelectrode and a Ag:AgCl loop around the end of the tube on which the membrane was formed. Current pulses were applied and the size of the potential jump measured before and after the membrane was advanced to cross the microelectrode tip. The larger the conductance, the smaller the difference between these two measurements. In our hands this method was not adequate for experiments with Cs which produces the highest single channel conductances of the ions investigated. When sufficient gramicidin was added to increase the water permeability, the potential difference across the membrane was too small relative to the potential difference between the voltage electrodes. The technique was therefore modified to use two microelectrodes and allow tangential observation of the membrane with an inverted microscope. With a fixed electrode separation of about 5 μ the potential difference produced between the electrodes was much smaller (e.g., 15 mV for 1 mA in 100 mM CsCl) and it was possible to resolve a clear jump (e.g., 2 mV) in the size of the responses to current pulses when the membrane was advanced across the tip of the nearer electrode. Our results for Na, Rb, and Cs confirm the conclusions reached by Dani and Levitt (1981) and extend the results to the three ions for which tracer flux data are also available. Dani and Levitt found 115 mM for Li, 69 mM for K and 2 mM for Tl, while we find 80 mM for Na, 40 mM for Rb, and 15 mM for Cs. The dissociation constants for the alkali cations fall in the expected sequence and are intermediate between those found in the two fits of the conductance and permeability data. These first ion dissociation constants are consistent with fits to the conductance data provided a second ion can enter an occupied pore.

Based on ^{13}C and ^{23}Na NMR of gramicidin in micelles made from dodecyl phosphatidylcholine, Jing, Prasad and Urry (1994) have recently reported first ion dissociation constants of 25 mM for Na, 17 mM for K, 12.5 mM for Rb and Cs, and 1 mM for Tl. These values imply somewhat stronger binding than found here. Jing et al. also report that a second Na ion can bind.

For Cs and gramicidin in phosphatidylcholine bilayers, Finkelstein and Andersen (1981) inferred $K_D = 30$ mmolal from flux-ratio exponents and the conductance-

concentration curve. A similar value has been found with monoglyceride membranes (M. Jones, D.S. Game, S.P. Moule and S.B. Hladky, unpublished). Thus, all methods of determination lead to the conclusion that two ions can be in the channel simultaneously with a first ion dissociation constant for Cs in the relatively small range of 12.5–30 mM. For Cs there is at present no need to modify the two-ion, four-state model. The results reported here for Na together with the small flux ratio exponents for Na (Procopio & Andersen, 1979; Andersen, 1984; M. Jones, D.S. Game, S.P. Moule and S.B. Hladky, unpublished) and the failure of Na to block fluxes of hydrogen ions through the channel (Heinemann & Sigworth, 1989) leave little doubt that exit from singly occupied pores is more rapid for this ion than predicted by the "slow exit" fit of the model to the conductance and permeability data (Urban et al., 1978, 1980). However, at the same time the dissociation constants for Na inferred from the water permeability and NMR measurements are smaller than expected if only one Na ion can enter the pore. For diphytanoyl phosphatidylcholine membranes, Finkelstein and Andersen (1981) inferred from flux-ratio measurements that a second Na ion cannot enter an occupied pore and calculated from the conductance-concentration relation $K_D = 310$ mmolal. Calculated in the same manner (see e.g., the Eadee-Hofstee plot in Hladky and Haydon, 1984), the value for Na with monoglyceride membranes is 370 mM. The discrepancy between 370 and 80 mM occurs even though both sets of data were obtained for gramicidin in the same environment, planar glyceryl mono-oleate + n-hexadecane membranes. There appears to be no means to reconcile all of these observations with either a prohibition of second ion entry or the two-ion, four-state model. The data for Rb show no sign of the stronger binding relative to Cs that would be needed to explain the finding by Schagina et al. (1983) that the flux ratio exponent at 0.1 M was 2.1 for Rb but only 1.6 for Cs.

For Na concentrations of 0.5 and 1 M, the calculated water permeabilities are less than expected assuming blockade by binding to a single site. This could be evidence for binding of more than one ion in the channel. However, these data were obtained either with a urea concentration of 0.5 M which is only half the osmotic concentration of the salt (2 × 0.5 M) or with 1 M urea. In the former case, the corrections are large and any error in procedure will have distorted the values, while in the latter visible portions of the membrane were sometimes observed to revert spontaneously to thick film. It is thus possible that the membrane area was less than the initial value and the volume flow was reduced even in those membranes for which reversion was not observed. We therefore do not attach any significance to this deviation from the simple binding equation.

Levitt et al. (1978) observed that the slope of the plots of potential vs. the square root of time decreased as

the ion concentration increased. They explained the decrease on the basis that the buildup of the concentration changes in the aqueous phases would reduce the osmotic driving force which in turn would reduce the streaming potential and hence the observed increase in potential. This effect should occur and has been taken into account in calculating the corrections (see calculations above). However, the variation in slope that we observe (Fig. 5) cannot be explained in this manner because (i) it is seen even comparing 1 mM with 10 and 30 mM salt while for these concentrations no significant reduction in osmotic driving force is expected, and (ii) at high ion concentrations the observed reduction in slope is much too large. If the reduction in slope were a result of a decrease in the streaming potential, then the entire streaming potential would have been eliminated in the first few minutes of flow which in turn would correspond to a halt in the osmotic flow. The variation in slope is more likely to result from a difference in natural convection produced close to the inside surface of the membrane. At low ion concentrations the concentration changes produced by the flow result in little change in density of the solution adjacent to the membrane relative to that far from the membrane, and thus little convection. At high ion concentrations the density changes will be much more marked, convection will occur and the accumulation of ions near the membrane will be spread over a greater distance from the membrane with a smaller concentration change at any position. This would produce a smaller change in potential as observed. In experiments to be reported elsewhere we have observed the concentration profile for KCl using ion-selective electrodes. It is indeed much shallower and extends much further from the membrane with concentrated solutions.

References

Andersen, O.S. 1984. Gramicidin channels. *Annu. Rev. Physiol.* **46**:531–548

Andrews, D.M., Manev, E.D., Haydon, D.A. 1970. Composition and energy relationships for some thin lipid films, and the chain conformation in monolayers at liquid-liquid interfaces. *Special Disc. Faraday Soc.* **1**:46–56

Dani, J.A., Levitt, D.G. 1981. Binding constants of Li, K, and Tl in the gramicidin channel determined from water permeability measurements. *Biophys. J.* **35**:485–499

Finkelstein, A., Andersen, O.S. 1981. The gramicidin A channel: A review of its permeability characteristics with special reference to the single file aspect of transport. *J. Membrane Biol.* **59**:155–171

Heineman, S.H., Sigworth, F.J. 1989. Estimation of Na⁺ dwell time in the gramicidin A channel. Na ions as blockers of H⁺ currents. *Biochim. Biophys. Acta* **987**:8–14

Hinton, J.F., Whaley, W.L., Shungu, D., Koeppe, R.E., Millet, F.S.

1986. Equilibrium binding constants for the group 1 metal cations with gramicidin-A determined by competition studies and ²⁰⁵Tl nuclear magnetic resonance spectroscopy. *Biophys. J.* **50**:539–544

Hladky, S.B. 1972. The Mechanism of Ion Conduction in Thin Lipid Membranes Containing Gramicidin A. Ph.D. Thesis, University of Cambridge

Hladky, S.B. 1983. Water and ions in pores. *Biophys. J.* **41**:47a (*Abstr.*)

Hladky, S.B. 1988. Gramicidin: conclusions based on the kinetic data. *Curr. Top. Membr. Transp.* **33**:15–33

Hladky, S.B., Haydon, D.A. 1972. Ion transfer across lipid membranes in the presence of gramicidin A. I. Studies of the unit conductance channel. *Biochim. Biophys. Acta* **255**:493–501

Hladky, S.B., Haydon, D.A. 1984. Ion movements in gramicidin channels. *Curr. Top. Membr. Transp.* **21**:327–372

Jing, N., Prasad, K.U., Urry, D.W. 1994. The determination of binding constants of micellar-packaged gramicidin A by ¹³C and ²³Na NMR. *Biophys. J.* **66**:A218 (*Abstr.*)

Levitt, D.G. 1984. Kinetics of movement in narrow channels. *Curr. Top. Membr. Transp.* **21**:181–197.

Levitt, D. G., Elias, S.R., Hautman, J.M. 1978. Number of water molecules coupled to the transport of sodium, potassium, and hydrogen ions via gramicidin, nonactin, and valinomycin. *Biochim. Biophys. Acta* **512**:436–451

Monoi, H. 1985. Nuclear magnetic resonance of 23Na ions interacting with the gramicidin channel. *Biophys. J.* **48**:643–662.

Neher, E., Sandblom, J., Eisenman, G. 1978. Ionic selectivity, saturation, and block in gramicidin A channels: II. Saturation behavior of single channel conductances and evidence for the existence of multiple binding sites in the channel. *J. Membrane Biol.* **40**:97–116

Procopio, J., Andersen, O.S. 1979. Ion tracer fluxes through gramicidin A modified lipid bilayers. *Biophys. J.* **25**:8a–0

Rosenberg, P.A., Finkelstein, A. 1978. Water permeability of gramicidin A treated lipid bilayer membranes. *J. Gen. Physiol.* **72**:341–350

Schagina, L.V., Grinfeldt, A.E., Lev, A.A. 1978. Interaction of cation fluxes in gramicidin A channels in lipid bilayer membranes. *Nature* **273**:243–245

Schagina, L.V., Grinfeldt, A.E., Lev, A.A. 1983. Concentration dependence of bidirectional flux ratio as a characteristic of transmembrane ion transporting mechanism. *J. Membrane Biol.* **73**:203–216

Urban, B.W. Hladky, S.B. 1979. Ion transport in the simplest single file pore. *Biochim. Biophys. Acta* **554**:410–429

Urban, B.W., Hladky, S.B., Haydon, D.A. 1978. The kinetics of ion movements in the gramicidin channel. *Fed. Proc.* **37**:2628–2632

Urban, B.W., Hladky, S.B., Haydon, D.A. 1980. Ion movements in gramicidin pores. An example of single-file transport. *Biochim. Biophys. Acta* **602**:331–354

Urry, D.W., Trapane, T.L., Venkatachalam, C.M., McMichens, R.B. 1989. Ion interactions at membranous polypeptide sites using nuclear magnetic resonance: Determining rate and binding constants and site locations. *Methods Enzymol.* **171**:286–342

Wang, K.-W., Hladky, S.B. 1994. Absence of effects of low frequency, low amplitude magnetic fields on the properties of gramicidin A channels. **67**:1473–1483

Appendix

In the two-ion, four-state model for gramicidin it is presumed that almost all of the time an ion is within the pore it can be assigned to one end of the channel or the other. When that is the case the pore is almost always in one of four states: empty, occupied on the left, occupied on the right, or occupied by an ion at both ends. Conduction through this pore can then occur in two different modes. In the one-ion mechanism an ion enters an empty pore, crosses from one end to the other and then

emerges at the far end without encountering another ion. In the two-ion mechanism an ion enters, eventually moves to the far end, but it emerges after a second ion enters from the original side. It is important to emphasize the essential distinction between the effects of second ion entry and second ion occupancy. The two ion conduction mechanism requires a second ion to enter, but it does not require the channel to remain doubly occupied for very long as one or the other of the ions in the channel may quickly leave.

A correct "state" description would require states for each important occupancy state of the channel, which for up to two ions and perhaps ten water molecules would require a very large number of states (perhaps 3^{12}). Such a description is clearly not practical and would probably be useless. Instead it will be assumed that the states can be lumped into just five groups, corresponding to the occupancy states of the ions. The various water configurations within each of these groups is represented by an average.

The evolution of the model in time is described by the permitted transitions between the states as indicated in the Table. The steady-state solution is obtained from these equations by straight-forward algebra after setting the time derivatives of the probabilities of observing the states equal to zero. The original model is extended so that doubly occupied pores are allowed to be different depending upon the side from which the second ion enters the channel. This is intended to allow for the possibility that the number of water molecules between the ions might be a function of the osmolality of the solution to which the middle of the pore was last exposed.

$$\frac{dX_{00}}{dt} = B'X_{10} + B''X_{01} - (A'c' + A''c'')X_{00} \tag{A1}$$

$$\frac{dX_{01}}{dt} = A''c''X_{00} + k'X_{10} + E'X_{21} + E'^*X_{12} - (B'' + k'' + D'c')X_{01} \tag{A2}$$

$$\frac{dX_{10}}{dt} = A'c'X_{00} + k''X_{01} + E''X_{12} + E''^*X_{21} - (B' + k' + D''c'')X_{10} \tag{A3}$$

$$\frac{dX_{12}}{dt} = D''c''X_{10} - (E' + E''^*)X_{21} \tag{A4}$$

$$\frac{dX_{21}}{dt} = D'c'X_{01} - (E'' + E'^*)X_{12} \tag{A5}$$

$$1 = X_{00} + X_{01} + X_{10} + X_{12} + X_{21} \tag{A6}$$

Define the following combinations of constants:

$$\alpha' = \frac{A'c'B''}{A'c' + A''c''} + \frac{D'c'E''^*}{E' + E''^*} \tag{A7}$$

$$\alpha'' = \frac{A''c''B'}{A'c' + A''c''} + \frac{D''c''E'^*}{E'^* + E''} \tag{A8}$$

$$\beta' = \frac{B'}{A'c' + A''c''} + \frac{D'c''}{E'^* + E''} \tag{A9}$$

$$\beta'' = \frac{B''}{A'c' + A''c''} + \frac{D'c'}{E'' + E'^*} \tag{A10}$$

$$\Gamma = (k'' + \alpha')(1 + \beta') + (k' + \alpha'')(1 + \beta'') \tag{A11}$$

then

$$X_{10}(k' + \alpha'') = X_{01}(k'' + \alpha') \tag{A12}$$

$$X_{10}(1 + \beta') + X_{01}(1 + \beta'') = 1 \tag{A13}$$

For a symmetrical pore when there are no gradients

$$\Gamma = \frac{B}{Ac}\left(1 + \frac{2A}{B}c + \frac{AD}{BE}c^2\right)\left(k + \frac{B}{2} + \frac{D}{2}c\right) \tag{A14}$$

These relations lead to (with symmetrical, zero gradient limits in brackets)

$$X_{00} = \frac{B'(k'' + \alpha') + B''(k' + \alpha'')}{\Gamma(A'c' + A''c'')} \left(= \frac{1}{1 + \frac{2A}{B}c + \frac{AD}{BE}c^2}\right) \tag{A15}$$

$$X_{01} = \frac{k' + \alpha''}{\Gamma}\left(= \frac{A}{B}cX_{00}\right) \tag{A16}$$

$$X_{10} = \frac{k'' + \alpha'}{\Gamma}\left(= \frac{A}{B}cX_{00}\right) \tag{A17}$$

$$X_{12} = \frac{D'c'(k' + \alpha'')}{\Gamma(E'^* + E'')}\left(= \frac{AD}{2BE}c^2X_{00}\right) \tag{A18}$$

and

$$X_{21} = \frac{D''c''(k'' + \alpha')}{\Gamma(E' + E''^*)}\left(= \frac{AD}{2BE}c^2X_{00}\right) \tag{A19}$$

From these, one can calculate the flux of ions through a pore (in ions per second)

$$j_{ion} = k'X_{10} - k''X_{01} = \frac{\alpha'k' - \alpha''k''}{\Gamma} \tag{A20}$$

$$j_{ion} = \frac{A'B''k' - A''B'k''}{\Gamma(A' + A'')} + \frac{D'cE''^*k'}{\Gamma(E' + E''^*)} - \frac{D''cE'^*k''}{\Gamma(E'^* + E'')} \tag{A21}$$

It is also helpful in later calculations to note that the numbers of ions that cross the left- and right-hand ends of the pore by the one-ion mechanism are the same

$$A'c'X_{00} - B'X_{10} = B''X_{01} - A''c''X_{00} \tag{A22}$$

and similarly for the two-ion mechanism

$$D'c'X_{01} - E'^*X_{12} - E'X_{21} = E''X_{12} + E''^*X_{21} - D''c''X_{10} \tag{A23}$$

With no osmotic gradient, the distinction between X_{12} and X_{21} disappears, i.e., $E' = E'^*$ and $E'' = E''^*$ and the principle of microscopic reversibility requires for this model (see e.g., Urban & Hladky, 1979)

$$\frac{A'B''k'}{A''B'k''} = \frac{D'E''k'}{D''E'k''} = e^{\frac{zF\Delta\psi}{RT}} \tag{A24}$$

WATER FLUX ACROSS A SURFACE NORMAL TO THE AXIS OF THE PORE

Using the partial water fluxes indicated in the Table, the steady-state water flux through a pore (in molecules per second) is related to the rate constants and states of the two-ion model as follows:

$$j_{wc} = \mathscr{A}P_o X_{00}\Delta C_{osm} + \eta_A'(A'c'X_{00} - B'X_{10}) + \eta_A''(B''X_{01} - A''c''X_{00})$$
$$+ \eta_D'(D'c'X_{01} - E'X_{21}) - \eta_D'^*E'^*X_{12} + \eta_D''(E''X_{12} - D''c''X_{10})$$
$$+ \eta_D''^*E''^*X_{21} + \eta_k(k'X_{10} - k''X_{01}) \tag{A25}$$

where $\mathscr{A}$ is Avogadro's number, ΔC_{osm} is the difference between the total solute concentrations (permeant plus impermeant) on the two sides of the membrane, and P_o is the water permeability of a channel not containing any ions. Combining the above with (A22) and (A23):

$$j_{wc} = \mathscr{A}P_o X_{00}\Delta C_{osm} + (\eta_A' + \eta_A'')(A'c'X_{00} - B'X_{10}) + (\eta_D'$$
$$+ \eta_D'')(D'c'X_{01} - E'X_{21} - E'^*X_{12}) - (\eta_D'^* - \eta_D')E'^*X_{12}$$
$$+ (\eta_D''^* - \eta_D'')E''^*X_{21} + \eta_k(k'X_{10} - k''X_{01}) \tag{A26}$$

ELECTRO-OSMOSIS

With no osmotic gradient and no gradient of permeant ion,

$$\eta_D'^* = \eta_D'^*, \eta_D''^* = \eta_D'', E' = E'^*, E'' = E''^*, c' = c'' = c, \tag{A27}$$

$$A'cX_{00} - B'X_{10} = \frac{A'B''k' - A''B'k''}{\Gamma(A' + A'')}, \tag{A28}$$

$$D'X_{01} - E'X_{11} = \frac{D'cE''k' - D''cE'k''}{\Gamma(E' + E'')}, \tag{A29}$$

and

$$j_{ion} = k'X_{10} - k''X_{01} = \frac{A'B''k' - A''B'k''}{\Gamma(A' + A'')} + \frac{D'cE''k' - D''cE'k''}{\Gamma(E' + E'')}. \tag{A30}$$

Using these relations the water flux equation can be rewritten as

$$j_{wc} = \eta_s\left(\frac{A'B''k' - A''B'k''}{\Gamma(A' + A'')}\right) + \eta_d\left(\frac{D'cE''k' - D''cE'k''}{\Gamma(E' + E'')}\right) \tag{A31}$$

where

$$\eta_s = \eta_A' + \eta_A'' + \eta_k \tag{A32}$$

is the number of water molecules to pass through the pore when an ion traverses the pore by the single-ion mechanism and

$$\eta_d = \eta_D' + \eta_D'' + \eta_k \tag{A33}$$

is the corresponding number for the double-ion mechanism. The observable quantity thus depends only on the numbers of water molecules transported across the membrane in each mode and not on the proportions of this movement coupled to each step in the transport process.
Defining

$$\eta = \frac{J_{wc}}{J_{ion}} \tag{A34}$$

$$\eta = \eta_s + (\eta_d - \eta_s)\frac{Fc}{1 + Fc} \tag{A35}$$

where

$$F = \left(\frac{D'E''k' - D''E'k''}{A'B''k' - A''B'k''}\right)\left(\frac{A' + A''}{E' + E''}\right) \tag{A36}$$

For small applied potentials and a symmetrical pore the conditions

given above for microscopic reversibility can be used to simplify these relations to

$$F = \frac{D}{B} \tag{A37}$$

$$\eta = \frac{B\eta_s + Dc\eta_d}{B + Dc} \tag{A38}$$

Thus the transition from η_s to η_d depends on the relative rates of first ion exit and second ion entry and not on the second ion binding constant.

STREAMING POTENTIAL AND DEPENDENCE OF FLUXES ON OSMOTIC GRADIENTS

The streaming potential, $\Delta\psi$, is the potential for which the current, I, is zero in the presence of an osmotic gradient,

$$\Delta\pi = RT\Delta C_{osm}. \tag{A39}$$

Levitt et al. (1978) have shown using irreversible thermodynamics that

$$\left(\frac{\Delta\psi}{\Delta\pi}\right)_{I=0} = -\frac{\overline{V_w}}{zF}(\eta + 1) \tag{A40}$$

where $\overline{V_w}$ is the partial molar volume of water. This relation may be used to derive the dependence of the key combinations of the rate constants on the osmotic gradient. For low ion concentrations, the second and third terms in Eq. (A21) are negligible and thus for given ΔC_{osm} with the potential at the streaming potential, the difference, $A'B''k' - A''B'k''$, must be zero, i.e.,

$$\frac{A'B''k'}{A''B'k''} = 1 \tag{A41}$$

For sufficiently small osmotic and potential gradients (i.e., in the range of validity of irreversible thermodynamics) the changes in this ratio can be written as the sum of the changes due to the separate gradients

$$\delta\left(\frac{A'B''k'}{A''B'k''}\right) = \delta_{elec}\left(\frac{A'B''k'}{A''B'k''}\right) + \delta_{osm}\left(\frac{A'B''k'}{A''B'k''}\right) \tag{A42}$$

where δ_{elec} is calculated with no osmotic gradient and δ_{osm} is calculated with no electrical gradient. At the streaming potential these changes must be equal and opposite.
The change resulting from the potential difference follows immediately from (A24).

$$\delta_{elec}\left(\frac{A'B''k'}{A''B'k''}\right) = \frac{zF\Delta\psi}{RT} \tag{A43}$$

and thus at the streaming potential

$$\delta_{osm}\left(\frac{A'B''k'}{A''B'k''}\right) = -\frac{zF\Delta\psi_s}{RT} = \overline{V_w}(\eta_s + 1)\Delta C_{osm} \tag{A44}$$

Because the left- and right-hand side terms of this expression are independent of the potential for any small osmotic and electrical gradients

$$\delta\left(\frac{A'B''k'}{A''B'k''}\right) = \frac{zF\Delta\psi}{RT} + \overline{V_w}(\eta_s + 1)\Delta C_{osm}. \tag{A45}$$

and

$$A'B''k' - A''B'k'' = A''B'k'' \left(\frac{A'B''k'}{A''B'k''} - 1 \right)$$

$$\cong A''B'k'' \left(\frac{zF\Delta\psi}{RT} + \overline{V_w}(\eta_s + 1)\Delta C_{osm} \right) \tag{A46}$$

Similarly at high permeant ion concentrations (the same on both sides) the first term on the right of Eq. (A21) is negligible and thus

$$\frac{D'cE''^*k'/(E' + E''^*)}{D''cE'^*k''/(E'^* + E'')} = 1 \tag{A47}$$

and by the same arguments as before

$$\frac{D'cE''^*k'}{(E' + E''^*)} - \frac{D''cE'^*k''}{(E'^* + E'')} = \frac{D''cE'^*k''}{(E'^* + E'')} \left(\frac{zF\Delta\psi}{RT} + \overline{V_w}(\eta_d + 1)\Delta C_{osm} \right) \tag{A48}$$

As required for consistency, the ion flux calculated from Eqs. (A21), (A46) and (A48) for intermediate concentrations is zero when the potential equals the streaming potential calculated from Eqs. (A35), (A36), (A39) and (A40).

Open Circuit Water Flux for a Symmetrical Pore and Small Gradients

For $I = 0$, the net fluxes of ions across each end and the middle of the pore are zero. Thus, for the same permeant ion concentration on the two sides

$$A'cX_{00} - B'X_{10} = -(D'cX_{01} - E'^*X_{12} - E'X_{21}) \tag{A49}$$

$$A''cX_{00} - B''X_{01} = -(D''cX_{10} - E''^*X_{21} - E''X_{12}) \tag{A50}$$

and

$$k'X_{10} = k''X_{01} \tag{A51}$$

These may be used together with Eqs. (A1) to (A6) to solve for the state probabilities for a symmetrical pore and small electrical and osmotic gradients,

$$X_{00} = \frac{1}{1 + \dfrac{2A}{B}c + \dfrac{AD}{BE}c^2} \tag{A52}$$

$$X_{01} = \frac{k'(A' + A'')c}{k'B'' + k''B'}X_{00} \qquad X_{10} = \frac{k''(A' + A'')c}{k'B'' + k''B'}X_{00} \tag{A53}$$

$$X_{21} = \frac{k'(A' + A'')c}{k'B'' + k''B'} \left(\frac{D'c}{E' + E''^*} \right)X_{00} \tag{}$$

$$X_{12} = \frac{k''(A' + A'')c}{k'B'' + k''B'} \left(\frac{D''c}{E'' + E'^*} \right)X_{00} \tag{A54}$$

where rate constants without primes represent the values for no gradients. Using (A49) and (A50) the water flux equation (A26) can be rewritten as

$$J_{wc} = \mathcal{A}P_oX_{00}\Delta C_{osm} + (\eta'_A + \eta''_A - \eta'_D - \eta''_D)(A'cX_{00} - B'X_{10})$$
$$- (\eta''^*_D - \eta'_D)E''^*X_{12} + (\eta''^*_D - \eta'_D)E''^*X_{21} \tag{A55}$$

The second factor in the second line of this equation can be rewritten using in turn (A53), (A46), (A39), (A40) and (A38)

$$A'cX_{00} - B'X_{10} = \frac{A'B''k' - A''B'k''}{k'B'' + k''B'}cX_{00}$$
$$= \frac{Ac}{2} \left(\frac{zF\Delta\psi_{st}}{RT} + \overline{V_w}(\eta_s + 1)\Delta C_{osm} \right)X_{00}$$
$$= \frac{ADc^2(\eta_s - \eta_d)}{2(B + Dc)}\overline{V_w}\Delta C_{osm}X_{00} \tag{A56}$$

Similarly, the third line of (A55) can be rewritten making use of the general algebraic relation

$$ax - by = \frac{(a - b)(x + y) + (a + b)(x - y)}{2} \tag{A57}$$

and then (A54), (A48), (A40), (A39) and (A38) with the result

$$(\eta''^*_D - \eta'_D)E''^*X_{21} - (\eta''^*_D - \eta'_D)E'^*X_{12} \tag{A58}$$
$$= (\eta''^*_D - \eta'_D - \eta''^*_d + \eta'_D)\frac{AD}{2B}c^2X_{00}$$
$$+ (\eta''^*_D - \eta'_D + \eta''^*_D - \eta'_D)\frac{ADc^2(\eta_d - \eta_s)}{4(B + Dc)}\overline{V_w}\Delta C_{osm}X_{00} \tag{A58}$$

Combining (A55), (A56) and (A58)

$$J_{wc} = \mathcal{A}P_oX_{00}\Delta C_{osm} + (\eta_s - \eta_d)^2\frac{ADc^2}{2(B + Dc)}\overline{V_w}\Delta C_{osm}X_{00}$$
$$+ (\eta'_D - \eta'_d)\frac{AD}{2B}c^2X_{00} \tag{A59}$$

where

$$\eta'_d = \eta'_D + \eta''^*_D + \eta_k \tag{A60}$$

$$\eta''_d = \eta''_D + \eta''^*_D + \eta_k \tag{A61}$$

and

$$\eta_d = \frac{\eta'_d + \eta''_d}{2}. \tag{A62}$$

It should be noted that the assumption of sufficiently small gradients requires that

$$\eta'_d + \eta''_d \gg \eta'_d - \eta''_d \tag{A63}$$

Short-Circuit Fluxes

It can be shown directly from the equation for the ion flux that the short-circuit current with an osmotic gradient is just the streaming potential times the membrane conductance. Somewhat more algebra is required, but it is also possible to show that the difference between the short-circuit and open-circuit water fluxes is just the short-circuit current times η.